Supporting Information

Bismuth Dots Imbedded in Nitrogen-Doped Carbon Nanotubes for Highly Efficient Lithium Ion Storage

Xiaoling Qiu,[a] *Boya Wang,*[a] *Peng Jing,*[a] *Yin Zhang,*[a] *Mi Zhang,*[b] *Qian Wang,*[a] *Xianchun Chen,**[,a] *Yun Zhang,*[a] *Hao Wu**[,a]

[a] College of Materials Science and Engineering, Sichuan University, Chengdu, Sichuan, 610064, P. R. China.

[b] College of Chemistry, Sichuan University, Chengdu, Sichuan, 610064, China.

[*] Corresponding author (email: chenxianchun@scu.edu.cn; hao.wu@scu.edu.cn)

Supporting Figures and Tables

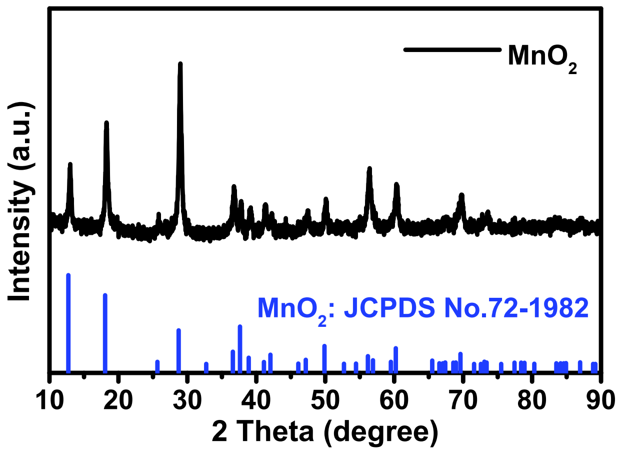

Fig. S1 XRD patterns of MnO_2.

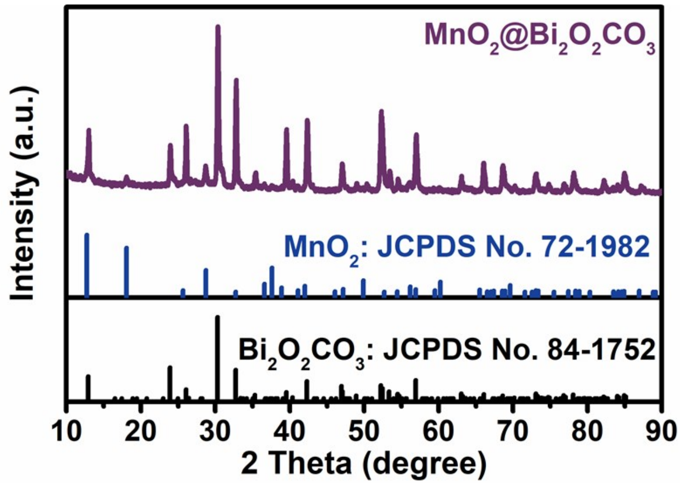

Fig. S2 XRD patterns of $MnO_2@Bi_2O_2CO_3$ (sample-2).

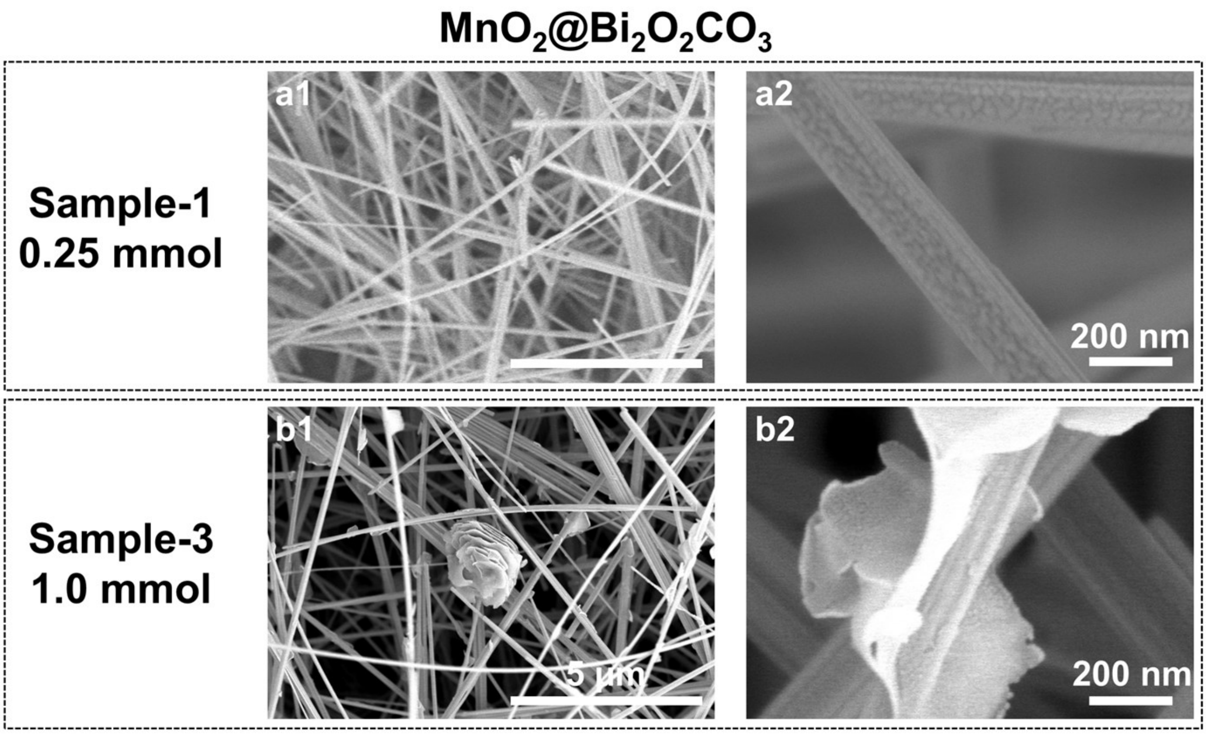

Fig. S3 SEM images of MnO_2@$Bi_2O_2CO_3$ with different amount of $Bi(NO_3)_3{\cdot}5H_2O$: (a1 and a2) 0.25 mmol and (b1 and b2) 1.0 mmol.

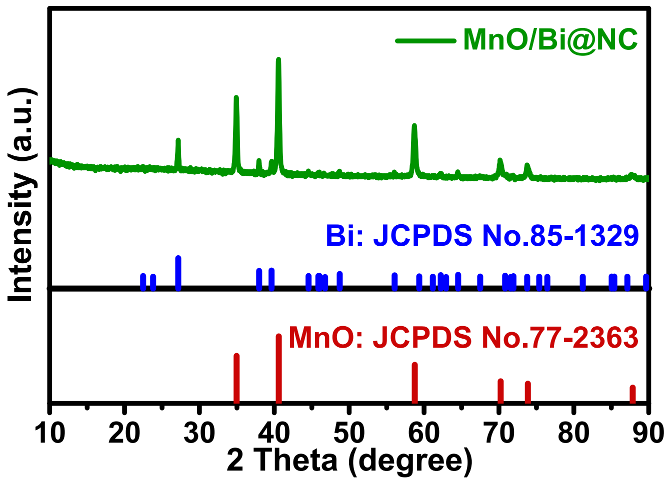

Fig. S4 XRD patterns of MnO/Bi@NC.

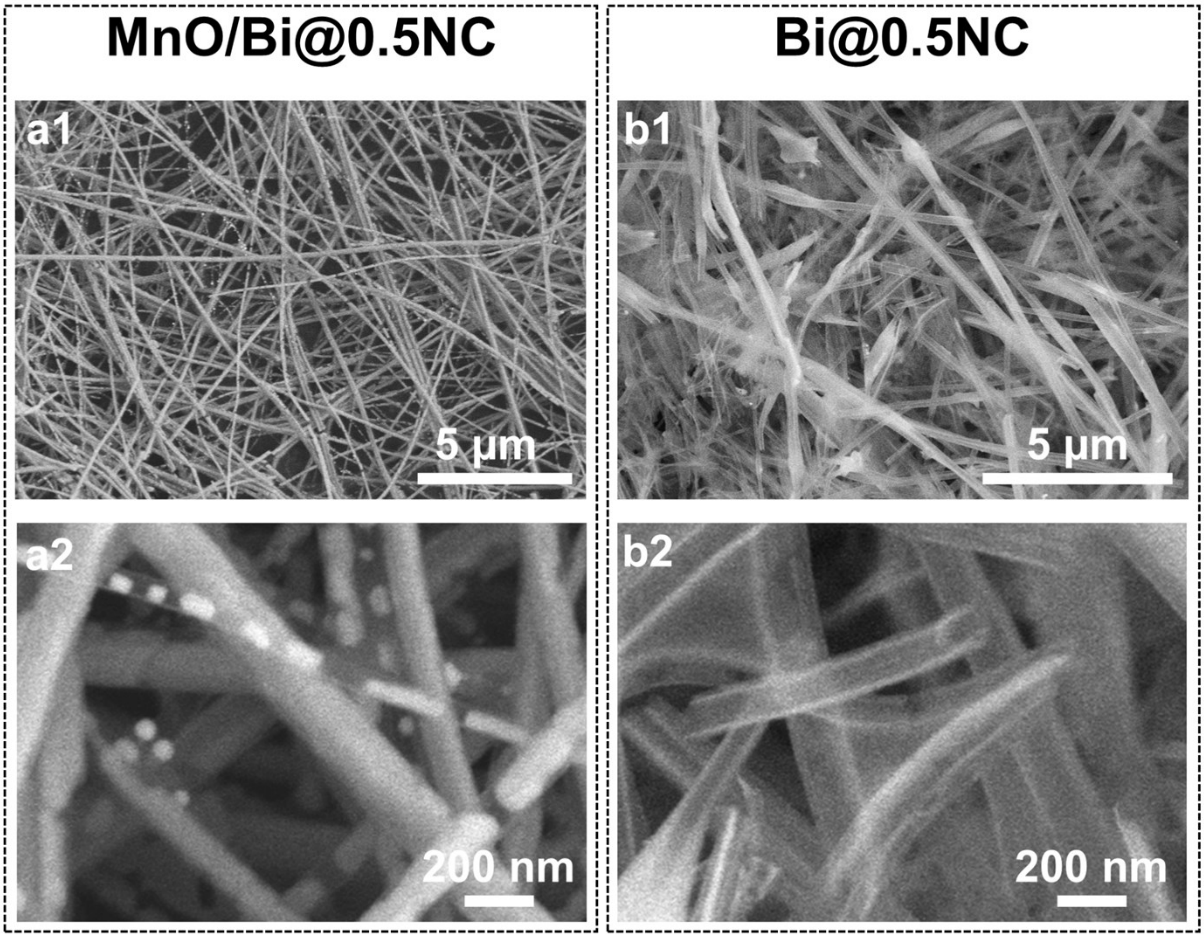

Fig. S5 SEM images of (a1 and a2) MnO/Bi@0.5NC and (b1 and b2) Bi@0.5NC.

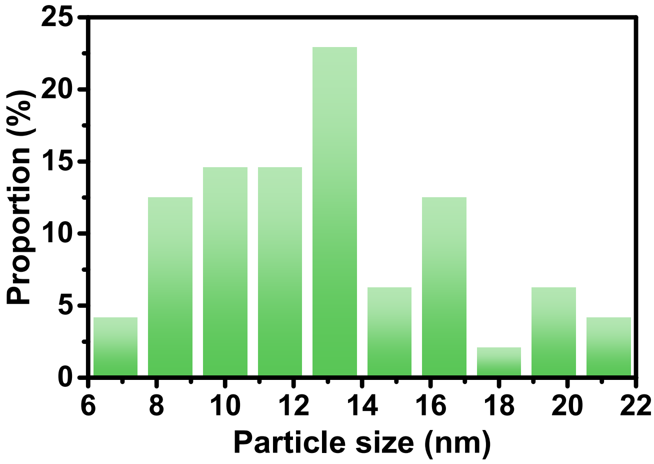

Fig. S6 Particle size distribution of Bi@NC.

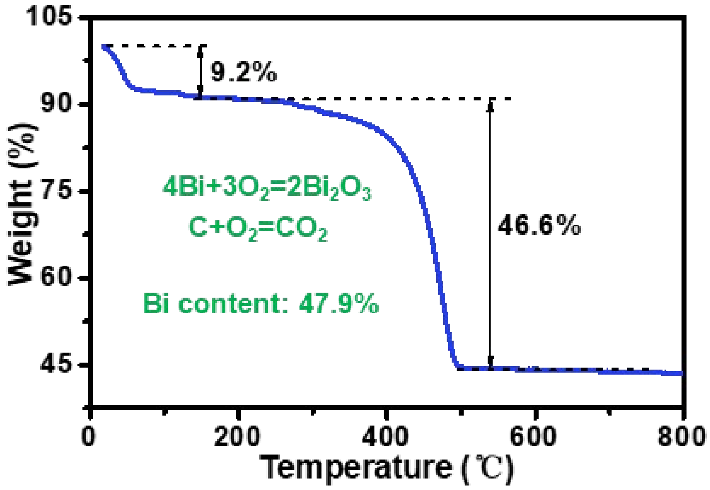

Fig. S7 TGA curve of the Bi@NC.

The Bi content is determined by the following equation:

$$Bi\ (wt\%) = 100 \times \frac{2 \times molecular\ weight\ of\ Bi}{molecular\ weight\ of\ Bi_2O_3} \times \frac{final\ weight\ of\ Bi_2O_3}{initial\ weight\ of\ Bi@NC}$$

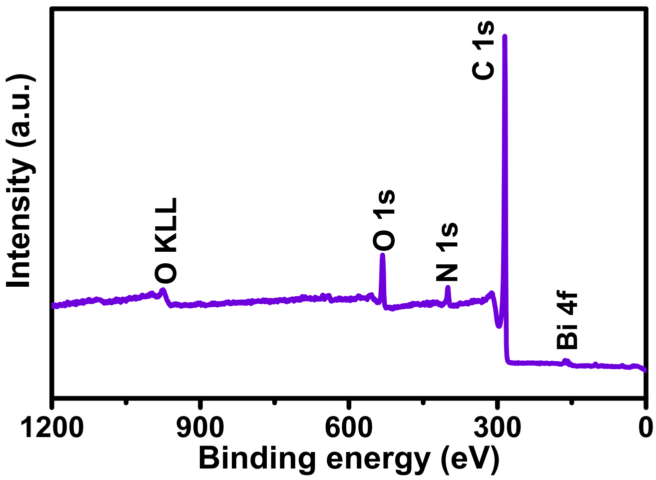

Fig. S8 XPS survey spectrum of Bi@NC.

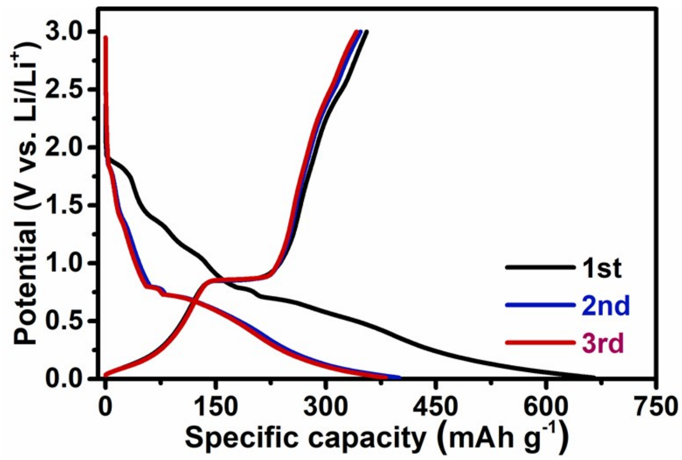

Fig. S9 The initial three charge/discharge profiles of CNT@Bi.

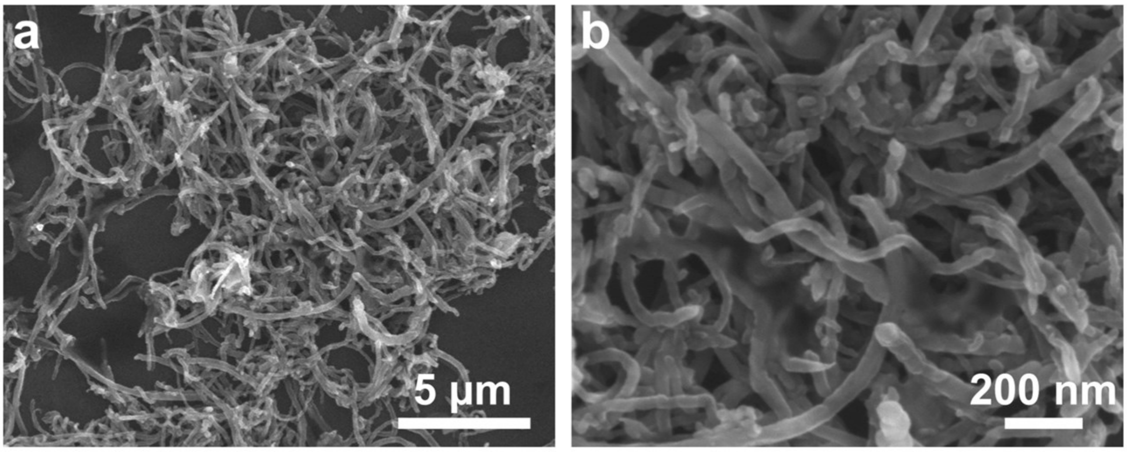

Fig. S10 SEM images of CNT@Bi.

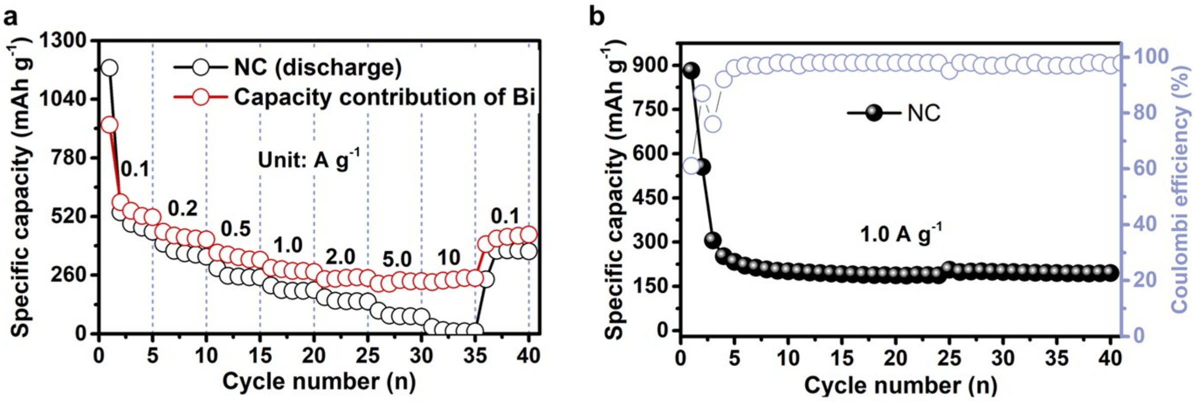

Fig. S11 (a) Rate capacity performance of NC and the corresponding capacity contribution of Bi in Bi@NC hybrid. (b) Cycling performance of the NC at 1.0 A g^{-1}.

The capacity contribution of Bi in Bi@NC was calculated based on the following formula:

$$C_{Bi}\left(mAh\ g^{-1}\right) = \frac{C_{Bi@NC} \times m_{Bi@NC} - C_{NC} \times m_{NC} \times w_{NC}}{w_{Bi@NC}}$$

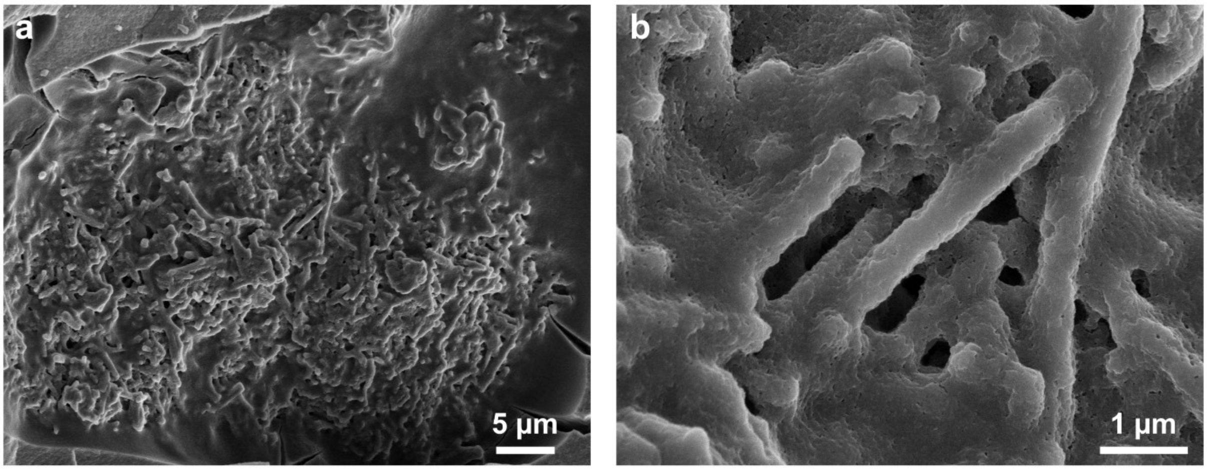

Fig. S12 SEM images of Bi@NC electrode after 2000 cycles at 1.0 A g^{-1}.

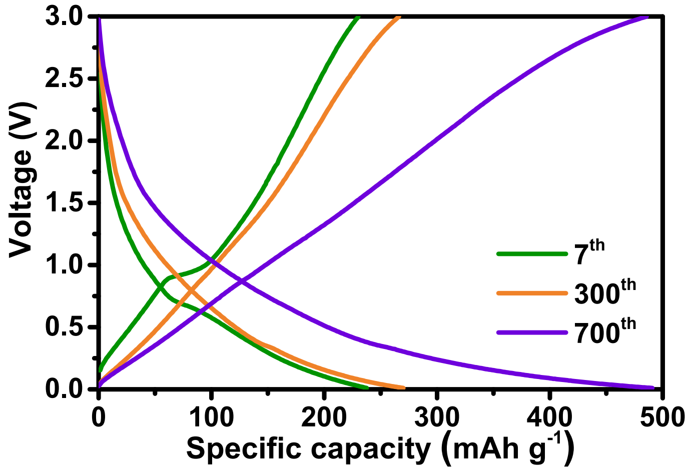

Fig. S13 Charge/discharge curves of the Bi@NC at selected cycles.

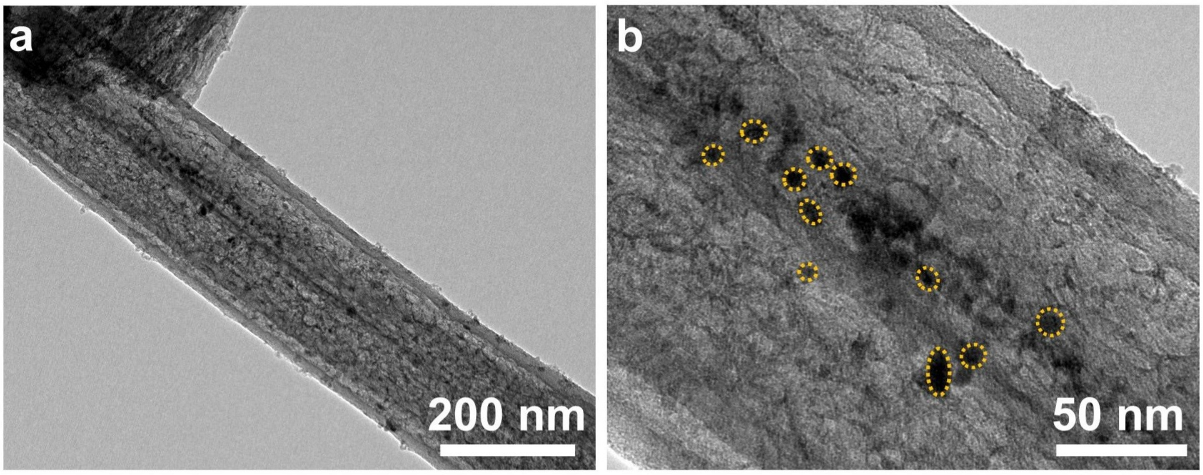

Fig. S14 TEM images of (a and b) Bi@NC electrode after 180 cycles at 1.0 A g^{-1}.

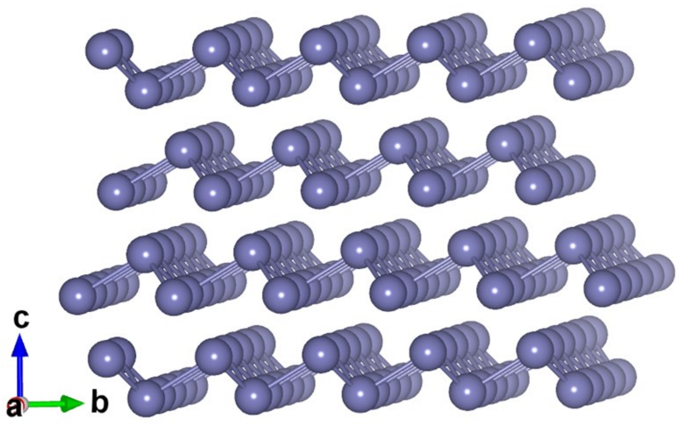

Fig. S15 Typical structure model of the optimized (001) crystal plane of Bi.

Table S1 A comparison of Bi-based materials for LIBs.

Electrode	Cyclability (capacity retention (mA h g^{-1}) @ cycle number) at current density	Rate performance (mAh g^{-1}) at (Y) current density (mA g^{-1})	References
Bi@NC	285 @ 100 at 100 mA g^{-1}	100 (3840)	1
Bi@C microsphere	280 @ 100 at 100 mA g^{-1}	90 (2000)	2
$Bi/Al_2O_3/C$ nanocomposite	310 @ 100 at 100 mA g^{-1}	——	3
Bi/C nanofibers	316 @ 500 at 100 mA g^{-1}	159 (3200)	4
Yolk−shell Bi@C−N	300 @ 500 at 1000 mA g^{-1}	289 (2000)	5
Bi/CNFs	483 @ 200 at 100 mA g^{-1}	170 (2000)	6
Bi@C core–shell (nanowires)	408 @ 100 at 100 mA g^{-1}	240 (1000)	7
Rose-like Bi@NC	535 @ 450 at 200 mA g^{-1}	250 (1000)	8
Bi/C composite sheets	315 @ 1000 at 1000 mA g^{-1}	99 (10000)	9
Bi@PC	380 @ 500 at 500 mA g^{-1}	215 (2000)	10
Bi@NC	**470 @ 2000 at 1000 mA g^{-1}**	**117 (10000)**	**This work**

Table S2 Lattice parameters and calculated surface energies of Bi with different orientations.

Surface	Lattice parameters (Å)	Surface energy (J m^{-2})
(001)	a = 9.92, b = 9.92	0.18
(101)	a = 14.94, b = 9.92	0.26
(110)	a = 11.86, b = 15.74	0.39
(111)	a = 14.94, b= 14.94	0.35
(211)	a = 19.71, b = 14.94	0.31
(221)	a = 15.74, b = 25.41	0.34
(201)	a = 25.40, b = 9.09	0.40
(210)	a = 11.86, b = 24.03	0.33
(212)	a = 14.97, b = 21.72	0.49
(102)	a = 19.71, b = 9.09	0.57

References

1. Y. T. Zhong, B. Li, S. M. Li, S. Y. Xu, Z. H. Pan, Q. M. Huang, L. D. Xing, C. S. Wang and W. S. Li, Bi nanoparticles anchored in N-doped porous carbon as anode of high energy density lithium ion battery, *Nano Micro. Lett.*, 2018, **10**, 56–69.
2. F. H. Yang, F. Yu, Z. Zhang, K. Zhang, Y. Q. Lai and J. Li, Bismuth nanoparticles embedded in carbon spheres as anode materials for sodium/lithium-ion batteries, *Chem. Eup. J.*, 2016, **22**, 2333–2338.
3. C.-M. Park, S. Yoon, S.-I. Lee and H.-J. Sohn, Enhanced electrochemical properties of nanostructured bismuth-based composites for rechargeable lithium batteries, *J. Power Sources*, 2009, **186**, 206–210.
4. H. Yin, Q. W. Li, M. L. Cao, W. Zhang, H. Zhao, C. Li, K. K. Huo and M. Q. Zhu, Nanosized-bismuth-embedded 1D carbon nanofibers as high-performance anodes for lithium-ion and sodium-ion batteries, *Nano Res.*, 2017, **10**, 2156–2167.
5. W. W. Hong, P. Ge, Y. L. Jiang, L. Yang, Y. Tian, G. Q. Zou, X. Y. Cao, H. S. Hou and X. B. Ji, Yolk–shell-structured bismuth@N-doped carbon anode for lithium-ion battery with high volumetric capacity, *ACS Appl. Mater. Interfaces*, 2019, **11**, 10829–10840.
6. Y. Q. Jin, H. C. Yuan, J. L. Lan, Y. H. Yu, Y. H. Lin and X. P. Yang, Bio-inspired spider-web-like membranes with a hierarchical structure for high performance lithium/sodium ion battery electrodes: the case of 3D freestanding and binder-free bismuth/CNF anodes, *Nanoscale*, 2017, **9**, 13298–13304.

7. R. Dai, Y. H. Wang, P. M. Da, H. Wu, M. Xu and G. F. Zheng, Indirect growth of mesoporous Bi@C core–shell nanowires for enhanced lithium-ion storage, *Nano Scale*, 2014, **6**, 13236–13241.

8. J. L. Lan, M. Y. Jin, C. J. Qin, Y. H. Yu and X. P. Yang, Bio-inspired rose-like Bi@nitrogen-enriched carbon towards high-performance lithium-ion batteries, *Energy Technol. Environ.*, 2017, **2**, 7178–7184.

9. H. C. Yuan, Y. Q. Jin, X. N. Chen, J. L. Lan, Y. H. Yu and X. P. Yang, Large-scale fabrication of egg-carton-inspired Bi/C composite toward high volumetric capacity and long-life lithium ion batteries, *ACS Sustainable Chem. Eng.*, 2019, **7**, 6033–6042.

10. W. W. Hong, A. Wang, L. Li, T. Y. Qiu, J. Y. Li, Y. L. Jiang, G. Q. Zou, H. J. Peng, H. S. Hou and X. B. Ji, Bi Dots Confined by Functional Carbon as High-Performance Anode for Lithium Ion Batteries, *Adv. Func. Mater.*, 2020, **30**, 2000756–2000765.